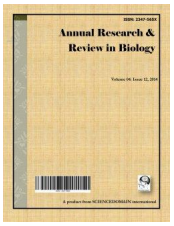

*Annual Research & Review in Biology*

*29(6): 1-14, 2018; Article no.ARRB.45687*
*ISSN: 2347-565X, NLM ID: 101632869*

# Reorganization of Actin Cytoskeleton and Microtubule Array during the Chondrogenesis of Bovine MSCs

**Anna A. Tvorogova[1,2], Anastasia V. Kovaleva[1,2] and Aleena A. Saidova[1,2*]**

*[1]Faculty of Biology, M. V. Lomonosov Moscow State University, Moscow, 119991, Russia.*
*[2]Center of Experimental Embryology and Reproductive Biotechnology, 127422, Moscow, Russia.*

***Authors' contributions***

*This work was carried out in collaboration with all the authors. Authors AAS and AAT conceived and designed the experiments. Authors AAS, AAT and AVK performed the experiments. Authors AAS, AAT and AVK analyzed the data. Authors AAS and AAT contributed to the writing of the manuscript.*

***Article Information***

DOI: 10.9734/ARRB/2018/45687
Editor(s):
(1) Dr. George Perry, Dean and Professor of Biology, University of Texas at San Antonio, USA.
Reviewers:
(1) Alessandro Poggi, IRCCS San Martino Hospital-IST, National Institute for Cancer Research, Italy.
(2) John Agbo, Abubakar Tafawa Balewa University, Nigeria.
Complete Peer review History: http://www.sciencedomain.org/review-history/27925

***Original Research Article***

***Received 06 October 2018***
***Accepted 10 December 2018***
***Published 22 December 2018***

## ABSTRACT

Mesenchymal stem cells (MSCs) are multipotent stem cells that are capable of self-renewal and can be committed into classical mesodermal tri-lineage differentiation (adipocytes, osteocytes and chondrocytes). During chondrogenic differentiation MSCs change their shape due to the reorganization of cytoskeletal components. This has been well documented for human and rodent models. Morphological changes of microtubule network and actin filaments that occur during the chondrogenic differentiation of MSCs from large animal models remain unknown. In this study we described the morphological changes of cell shape, area, actin structures and microtubule array that occur in bovine MSCs during the chondrogenic differentiation of bovine bone-marrow isolated MSCs. Chondrogenic differentiation of bMSCs occur more rapidly on glass substrate compared to the cells plated on vitronectin, and in 7 days after the commitment we observed clusters of small round-shaped cells that expressed glycosaminoglycans. During the differentiation microtubule (MT) array of MSCs became non-radial, and non-centrosomal MTs that grew transversely to the cell radius appeared in the inner cytoplasm and near the cell edges. At the end of differentiation process we observed the thick bundles of MTs that grew in parallel to the cell edge and basket-like

**Corresponding author: E-mail: saidova@mail.bio.msu.ru;*

structures of curved MTs around the nucleus. The main changes of actin structures in differentiating MSCs included the disappearance of thick transverse stress fibers and actin arches and reorganization of actin into chaotic network of thin cortical fibers. Our results imply the important role of both actin and MT cytoskeletal systems in chondrogenesis and reveals new perspectives for experimental regulation of these process *in vitro* systems.

*Keywords: MSC; chondrogenesis; cytoskeleton; actin; microtubules.*

## 1. INTRODUCTION

Mesenchymal stem cells are the group of adult multipotent stem cells that were first described by A.J. Friedenstein [1]. Bone marrow is the conventional source of MSC, however, they can also be derived from adipose tissue, peripheral blood, dermis, and fetal organs and fluids [2-5]. MSCs are defined as highly adherent cells with a spindle-like morphology that express the surface markers CD29, CD44, CD73, CD90, and CD105 and lack the expression of hematopoietic markers CD31, CD34 and CD45. Several studies confirmed the stemness of isolated MSCs by the expression of pluripotency markers, including Oct4, Sox 2 and Nanog. However, the data on the expression of these markers in MSC cells are controversial [3,6,7]. MSCs can differentiate into three conventional mesodermal lineages that include chondrocytes, adipocytes, and osteocytes both in vivo and in vitro [8]. However, the plasticity of MScs is not limited to mesodermal lineages, as MSCs can also differentiate into hepatocytes and neurons, which are the derivatives of endodermal and ectodermal differentiation [9]. The differentiation capacities of MSCs depend on the chemical composition of culture media and the type of the adhesive substrate. Rigid substrates like graphene and rigid gels promote the osteogenic differentiation, while the soft substrates (like sort polyacrylates and fibroblast-produced ECM) can induce the spontaneous chondrogenic differentiation of MSCs even in the absence of chemically modified media [10,11]. During the differentiation process, MSCs rearrange the organization of the cytoskeleton, and become round-shaped in case of chondrogenic and adipogenic differentiation and form long protrusions when turning into the osteoblasts [12,13].

Cytoskeleton system of MSCs consists of three components, including the actin network, microtubules and intermediate filaments. Actin structures of MSCs are organized into long fine stress-fibers growing parallel to the extended cell axis [12,14]. Rearrangement of the actin cytoskeleton during the osteogenic differentiation occurs through the disruption of stress fibers in the cell body and the formation of thick actin bundles in the cell periphery. Disruption of the actin cytoskeleton with cytochalasin D prevents the osteogenic differentiation of MSCs and leads to the decrease of alkaline phosphatase activity and calcium deposition [12]. Microtubule system organization of MSCs is similar to that in fibroblasts and can be described as a radial array of long microtubules growing from centrosome [15]. During the osteogenic differentiation, MSCs retained the radial pattern of MTs, and no significant changes were reported for MT dynamics. In contrast to osteogenic differentiation, very few data are available for changes of actin and MT cytoskeleton during the chondrogenic MSC differentiation.

Changes in cytoskeleton system control the cell migration, division and respond external stimuli [16]. The interactions between cytoskeletal proteins and components of the extracellular matrix define the cell shape, adhesion, and even differentiation capacities [17,18]. Due to this fact, there is an increasing interest in the role of cytoskeletal components in MSc differentiation. In contrast to human MSC research, the changes of the cytoskeleton system during the differentiation of non-human MSc are still underexplored. Large animal models, including cattle, open new perspectives for regenerative medicine and translational research in the veterinary field [19-22]. Our main objective was to describe the changes of MT and actin cytoskeleton during the chondrogenic differentiation of bMSCs. This study will provide new clues on the relationship between bovine MSC differentiation and cytoskeleton and will get the new data of cytoskeleton changes during chondrogenesis.

## 2. MATERIALS AND METHODS

### 2.1 Cell Culture

Bovine MSCs (were provided by UNU "Collection of cell cultures" of the Center for Scientific Research and Development of the Russian

Academy of Sciences). Bovine MScs were isolated from the bone marrow of 4 Holstein calves. Cells were plated on the Petri dishes with the glass coverslips or glass coverslips coated with vitronectin ($5x10^{-6}$g/ml, Sigma-Aldrich Chemical Co. (St. Louis, MO, USA)) at a final concentration of $25x10^3$ cells/cm² in a humidified atmosphere of 37°C and 5% CO2. The chondrogenic medium consisted of high glucose DMEM, 1xITS, 1% gentamicin, 1% amphotericin, 50 mg/ml ascorbate, 10 ng/ml TGF-B1 and 100 nM dexamethasone. The medium for control cells was DMEM/F12 1:1 with 10% fetal bovine serum (Paneco, Russia), L-glutamine (Paneco, Russia), 1% gentamicin and 1% amphotericin. Cells at passage 4 were used in this study.

## 2.2 Immunofluorescence

Cells were fixed with ice-methanol (Merck KGaA, Germany) for 20 minutes at -20°C at days 1, 7, 14 and 21 and rinsed in 1x PBS. Microtubules were visualized by staining with primary alpha-tubulin antibody (clone DM1A, Invitrogen, USA) in 1:100 dilution for 60 min at 37°C and further staining with Cy2-labeled rabbit anti-mouse secondary antibody (Invitrogen, USA) 1:100 for 60 min at 37°C, cell nuclei were counterstained with DAPI (1:500) for 10 min at room temperature (RT). Fixed cells were imaged on Nikon Ti-E microscope under PlanApo x 20 or × 40/1.4 objective (phase contrast) with CoolSnapHQ digital camera using filter sets for FITC and DAPI. Stemness markers were visualized with the antibodies to Oct-4A (clone C30A3, Cell Signalling, USA), Nanog (clone 4903S, Cell Signalling, USA) and to Sox2 (clone 4900S, Cell Signalling, USA) with the same protocol.

To visualize actin network cells were fixed with 4% paraformaldehyde for 15 min at RT (Merck KGaA, Germany) and permeabilized with 1% Triton X-100 (Sigma Aldrich, USA) for 60 min at days 1, 7, 14 and 21. The F-actin cytoskeleton was visualized by ActinRed555 ReadyProbes reagent (Invitrogen by Thermo Fisher Scientific, USA), cell nuclei were counterstained with DAPI (1:500) for 10 min at RT. Fixed cells were imaged on Nikon Ti-E microscope under PlanApo x 20 or × 40/1.4 objective (phase contrast) with CoolSnapHQ digital camera using filter sets for TRITC and DAPI.

## 2.3 Histology

MSCs were fixed with ice-methanol and stained with Shandon Instant Hematoxylin (Thermo ELECTRON CORPORATION) for 4 min at RT and were washed three times with tap water; cell cytoplasm was stained with eosin (AppliChem Inc., USA) at RT for 5 min.

To confirm the chondrogenesis process cells were fixed with 4% paraformaldehyde and incubated with 0.1% Safranin O (water solution) at RT for 5 min, as reported previously [23] and then imaged using a Nikon Eclipse 80I at x4, x10 and x20 magnification.

## 2.4 RNA and cDNA

RNA was extracted from thawed suspensions of cells using the RNeasy Mini Kit (Qiagen, USA) according to the manufacturer's instructions. The RNA concentration was measured using a Nano Photometer (Implen, Germany), and its purity was assessed according to the A260/A280 and A260/A230 ratios. cDNA was transcribed using the ImProm-II AMV-Reverse Transcription Kit (Promega, USA) according to the manufacturer's instructions.

## 2.5 Primers and Real-time PCR

Real-time qPCR was further performed on CFX96 (Applied Biosystems, USA) cycler with Taq-polymerase in SYBR Green I buffer (Syntol, Russia). The reaction protocol included denaturation (95°C, 10 min), followed by 40 amplification cycles (95°C, 15 sec; 60°C, 30 sec; and 72°C, 60 sec). All samples were processed in triplicate. All primers were synthesized and HPLC-purified by Syntol (Russia). Primer sequences for gene expression were reported by Cortes et al. [24].

## 2.6 Data Normalization and Analysis

The data were normalized according to the method proposed by Vandesompele et al. [25]. GAPDH and B-ACTIN genes were taken for the calculation of the normalization factor. Microscopic data were analyzed in ImageJ program (NIH, Bethesda, USA). Cell areas were measured using the free-hand selection tool to outline the cell boundary, and the applied the "Area measurement" built-in plugin to measure cell area in pixels. These values were recalculated into $\mu m^2$ by multiplying on the equivalent pixel size value (1 pixel was equal to 0.406 $\mu m^2$ for our camera).

## 3. RESULTS

### 3.1 Characterization of bMSCs

Primary bMSCs isolated from the bone marrow began to elongate and exhibited spindle-like morphology within 24 hours after attachment. bMSCs were highly adhesive both to glass and vitronectin substrates. Isolated cells were cultured for 2 weeks in monolayer and used for the differentiation experiments on the passage 4.

Expression of stemness markers of bovine MSCs was confirmed by RT qPCR and immunofluorescence techniques. IF and RT qPCR results revealed the high expression level of Oct-4, Sox2, and Nanog both on mRNA and protein level (Fig. 1A). Expression of stemness markers did not change significantly within 4 passages (Fig. 1B). Immunofluorescent staining of bMSCs revealed the uniform expression pattern of Nanog in the nuclei of all cells, whereas expression of Oct4 and Sox2 was heterogeneous (Fig. 1D), and we could see the cells with weak and high expression of these markers in the total population. Expression of surface molecules on bMSCs was also confirmed with RT qPCR; we detected high mRNA levels for CD73, CD90 and CD105 and the lack of CD45 mRNA (Fig. 1C), that allowed to confirm the conventional phenotype of bMSC and the absence of hematopoietic precursors in the population of bone marrow-isolated bMSCs.

### 3.2 Morphological Heterogeneity of Bovine MSCs

Both on glass and vitronectin substrates bMSc retain the fibroblast morphology and can be described as spindle-like elongated cells with large round nucleus (Fig. 2). The differences between mean area values for cells on glass and vitronectin were statistically insignificant. At the same time, cell population on both substrates is highly heterogeneous and can be distinguished into two distinct subpopulations of small (mean area < 1800 $\mu m^2$) and large (mean area > 10000 $\mu m^2$) cells. The percentage of small cells on both substrates was from 70 to 80% (Fig. 3). In 24 hours after the induction of chondrogenic differentiation, the population of bMSCs was still heterogeneous on both substrates. Mean area values for small and large cells on vitronectin were similar to control values, while the mean area value for the subpopulation of small cells on glass increased to 2604±97 $\mu m^2$ (compared to 1878±84 $\mu m^2$ for control cells), and the percentage of small cells on glass decreased from 70.2 to 55.1%. Expression of glycosaminoglycans detected with Safranin O staining began on the 14 days after the commitment. Expression of aggrecan and collagen type II mRNA in bMSCs increased gradually from day 7 to day 21, and we detected no significant differences in mRNA expression between cells on different substrates (data not shown).

Formation of cell clusters specific for chondrogenic differentiation began at day 7 after the commitment of MSCs with the modified chondrogenic medium (Fig. 4 C-D). The area of cell clusters on glass was larger than for vitronectin-attached cells (Fig. 4 A-D), and Safranin O staining was also more prominent for the MSCs on a glass substrate (Fig. 4E-H). A number of clusters for differentiated chondrocytes was higher for bMSCs on glass (17 clusters on 10 fields compared to 8 clusters for vitronectin-plated cells).

Thus, the integrin-independent substrate (adhesive glass) enhances the process of chondrogenic differentiation of bovine MSCs, while vitronectin, as a substrate with integrin-specific ligands, is less applicable for cells committed to chondrogenic differentiation.

### 3.3 Microtubule System in bMSCs under Chondrogenic Differentiation

Microtubules (MTs) in bMSCs are organized in a radial array with MTs growing from the microtubule-organizing center to the cell edge, and most of MTs are oriented in parallel to the long cell axis. MT pattern in most of the control cells was perfectly radial near the centrosome and became more chaotic in the outer cytoplasm (Fig. 5). In some cells, we observed a population of MTs in the inner cytoplasm and near the cell edge that grew perpendicularly to the cell radius, so in these cells, MTs was organized in a non-radial pattern. We defined the radiality of the MT array on a qualitative level. Cell was considered to have a radial MT array if we could visualize at least one dense cluster of MTs growing from one center, and most of MTs grew towards the cell edge. Otherwise, we considered the cell to have a non-radial array. For all time points (1, 7, 14 and 21 days) and experimental conditions (vitronectin and regular glass substrates) we have evaluated the radiality of MT array for at least 50 cells.

The percentage of cells with non-radial pattern varied from 3.39% to 2.46% (day 1 to day 21) for cells on glass and was nearly the same for cells on vitronectin (which varied from 3.39% to 3.45%) (Fig. 6). Mean cell area values for the cells with non-radial MT array decreased compared to cells with radial MT pattern (2904±34 $\mu m^2$ vs. 5495±34 $\mu m^2$) and the values of elongation factor (EF) are also lower than for cells with radial MT pattern (1.51±0.07 for cells with non-radial MTs vs 1.82±0.07 for cells with radial MTs).

During the chondrogenic differentiation of bMSCs, the subpopulation of cells with non-radial MT array increased gradually from day 1 to day 21 (Fig. 7). On both substrates, we observed the clusters of bMSCs with microtubules organized in a non-radial chaotic pattern with thick bundles of MTs growing in different directions at non-centrosomal MTs growing in the inner cytoplasm and near the cell edge (Fig. 6). Cells that did not gather in clusters demonstrated a radially organized MT array. At the day 21, we observed a cluster of nearly round cells (mean EF for 20 cells was 1.15±0.22) with a basket-like MT array around the nucleus (Fig. 7). Percentage of cells with non-radial MT array increased faster for glass attached cells and was 31.13% by day 14, whereas the percentage of cells with non-radial MT pattern for cells on vitronectin increased to 33.93% only by day 21 (Fig. 6, Fig. 8).

Thus, the main changes in MT array of bovine MScs during chondrogenic differentiation are the loss of radial growth, chaotic MT pattern in the inner cytoplasm and near the cell edges and the presence of thick bundles that are not oriented towards the long cell axis.

### 3.4 Actin cytoskeleton in bMSCs under chondrogenic differentiation

Actin cytoskeleton organization of bMSCs in control is similar to all cells with a mesenchymal type of motility. Actin structures of bMSCs are organized into fine stress-fibers and fine strands, cortical actin, and actin arches. Thick actin bundles are localized near stabilized lateral cell edges and several stress fibers that grew in directions transverse to cell radius. Actin arches are present in a majority of control cells and can be in parallel or transverse to the long cell absence; actin arches are absent in a few non-polarized cells (data not shown). There were no differences in the organization of actin cytoskeleton in subpopulations of small and large cells both on glass and vitronectin substrates (Fig. 10).

During chondrogenic differentiation of bMSCs changes of actin cytoskeleton were observed only for a subpopulation of small round shaped-cells that gathered in clusters. In these cells we observed the rearrangement of actin cytoskeleton into network-like structures, cell arches and stress fibers disappeared, and only short actin bundles appeared through the cytoplasm and organized into a chaotic network (Fig. 11). The actin cytoskeleton of bMSCs changed gradually from day 7 and became completely rearranged at day 21. bMSCs that did not come into clusters retained the morphology and organization of actin cytoskeleton similar to control cells. The were no differences in the organization of actin cytoskeleton for vitronectin and glass-plated cells, but the clusters of round-shaped cells with disrupted actin network appeared on day 14 on the glass, and whereas clusters of differentiated chondrocytes for vitronectin-plated cells appeared only at day 21.

## 4. DISCUSSION

Because of the poor regenerative capacity of cartilage tissue, articular cartilage is one of the central subjects for regenerative medicine. Experimental assays on bovine MSC models included the osteoarthritis, cartilage regeneration, and induced chondrogenesis [26-28]. The major problem of in vitro chondrogenesis assays was that MSC-seeded scaffolds and constructs could not reach the mechanical characteristics of the native cartilage due to the absence of additional microenvironmental stimuli. It was natural to assume that mechanical stimulation could be the optimal strategy to overcome the limitations of in vitro assays, and Huang et al. [29] demonstrated that dynamic compression applied to rabbit MSC-seeded scaffolds shortly after the chondrogenic commitment enhanced the chondrogenesis by the activation of TGFIII-beta pathway and led to the significant increase in expression of chondrogenesis-associated markers like collagen type II and aggrecan.

Moreover, Kupcsik et al. [30] showed that dynamic compression could sufficiently stimulate MSC chondrogenesis in the absence of chemically modified media. These data were the first cue to the possible role of cytoskeletal components in MSC differentiation. The second evidence of the possible role of cytoskeleton

system in chondrogenesis came from the study by Park et al. [31] who revealed that MSCs on soft substrates are more committed to chondrogenic and adipogenic differentiation, while the increase of substrate stiffness induced myogenesis of human MSCs.

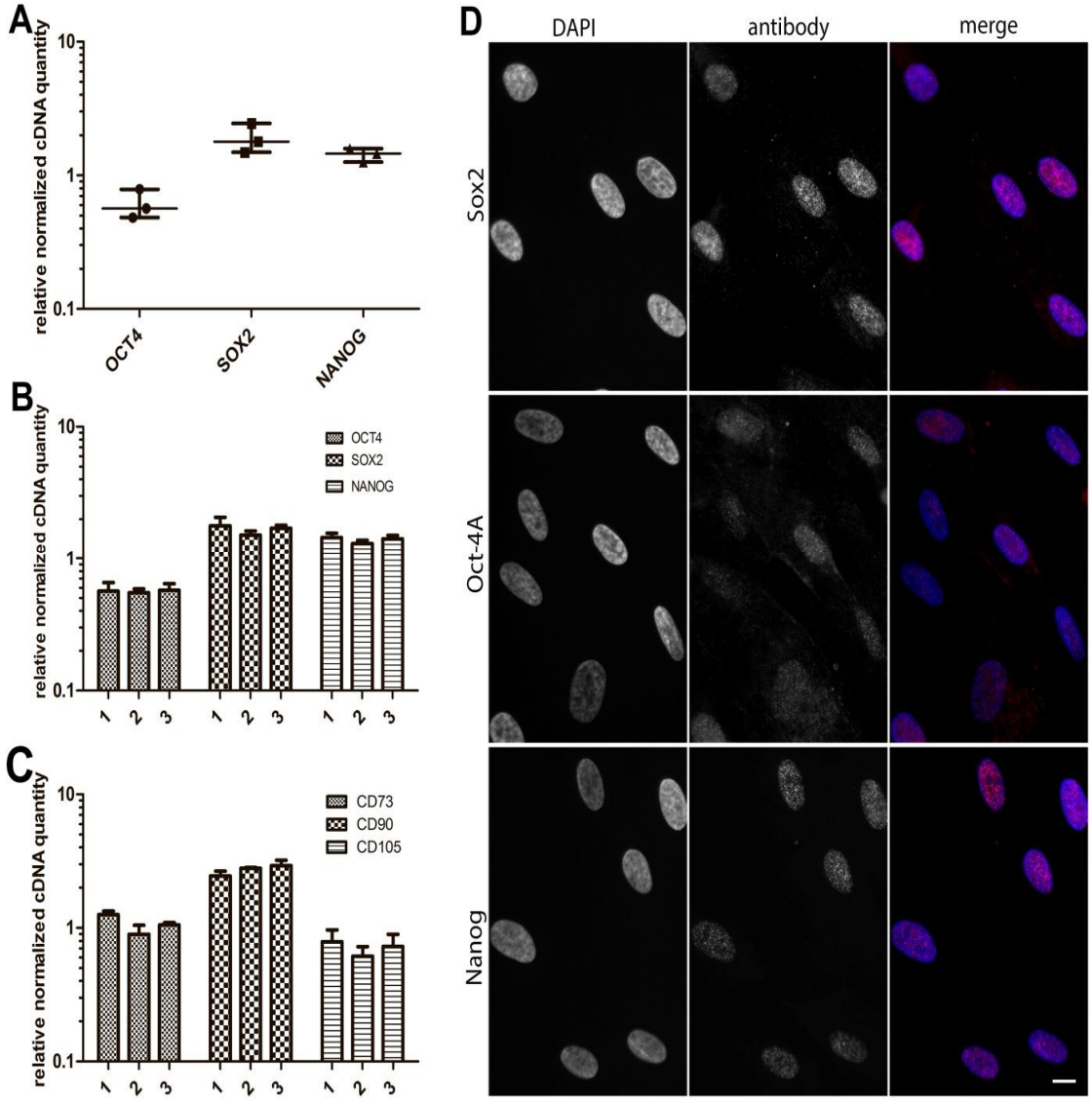


**Fig. 1. Expression of surface molecules and stemness markers in bone marrow-derived bMSCs**

*A – Normalized relative cDNA quantity of SOX2, OCT4 and NANOG in bMSCs of the first passage. All measurements were taken in triplicate, data were normalized for BACTIN and GAPDH, data are presented as median±range*

*B – Normalized relative cDNA quantity of SOX2, OCT4 and NANOG did not change significantly on 1, 2 and 3 passages*

*C - Normalized relative cDNA quantity of CD73, CD90 and CD105 in bMSCs from passages 1 to 3. All measurements were taken in triplicate, data were normalized for BACTIN and GAPDH, data are presented as mean±SEM*

*D - Immunofluorescent staining of bMSCs with antibodies to Oct4, Sox2 and Nanog, bar 10 μm. Nanog and Sox2 are expressed uniformly, while the expression of Oct4 is heterogeneous in population*

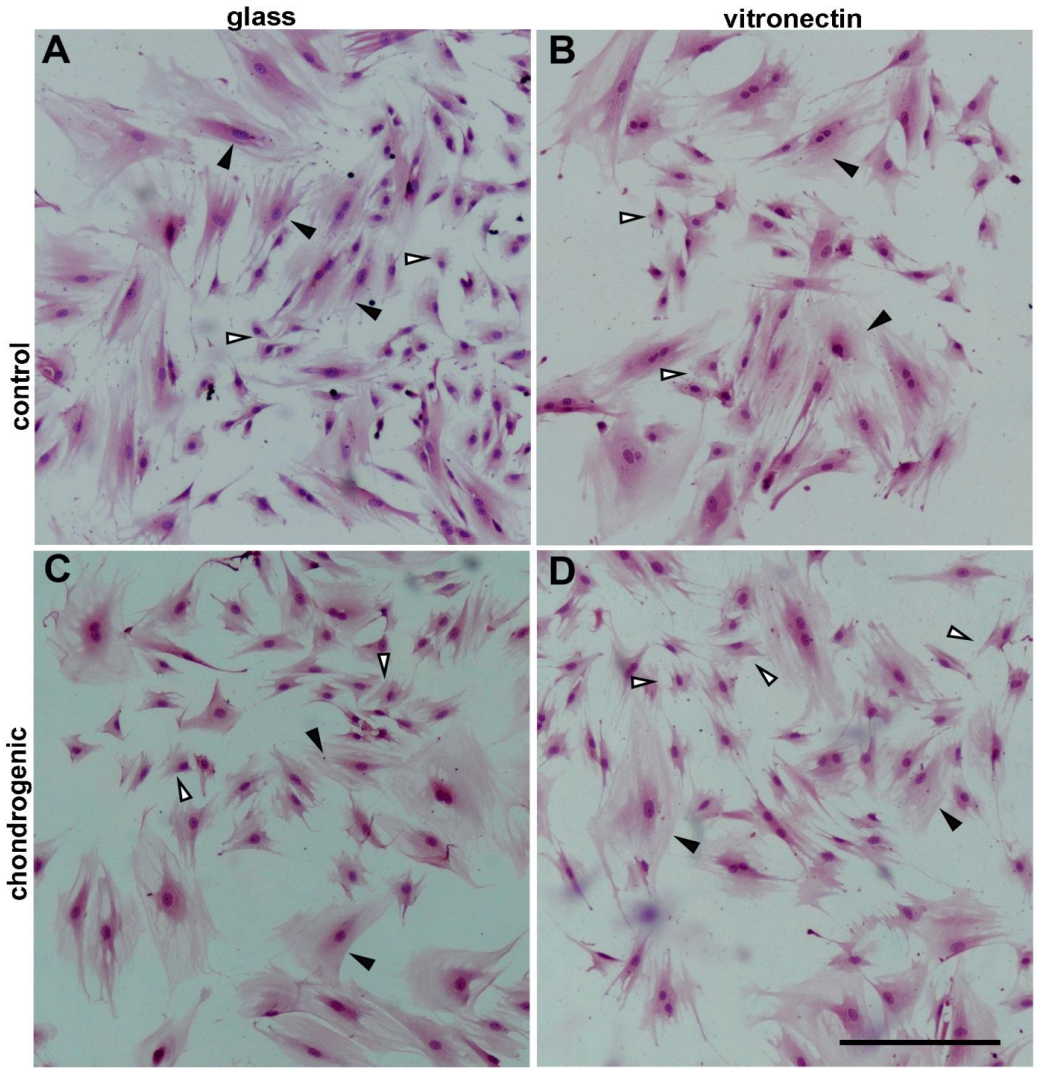


**Fig. 2. Heterogeneity of bMSCs population, staining with hematoxylin-eosin, bar 50 μm**

*A, C – cells plated on glass in control and chondrogenic media; B, D – cells plated on vitronectin in control and chondrogenic conditions. White triangles point the small cells subpopulation, black triangles point the subpopulation of large cells*

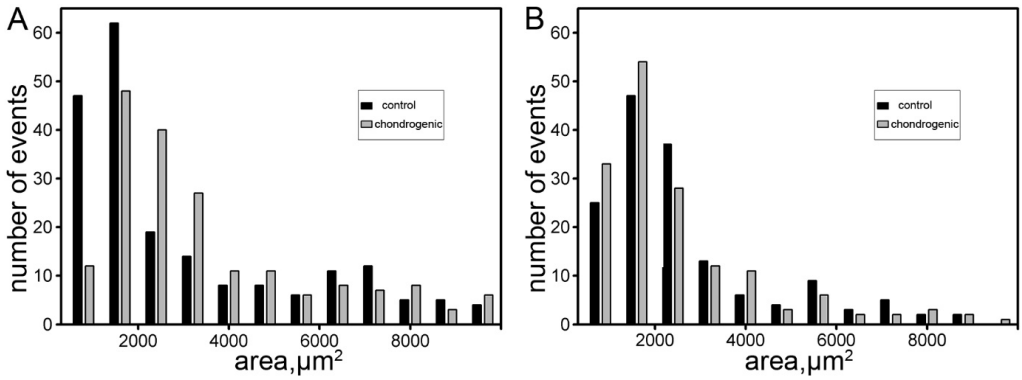


**Fig. 3. Histograms of mean cell area for MSCs plated on vitronectin (A) and glass (B)**

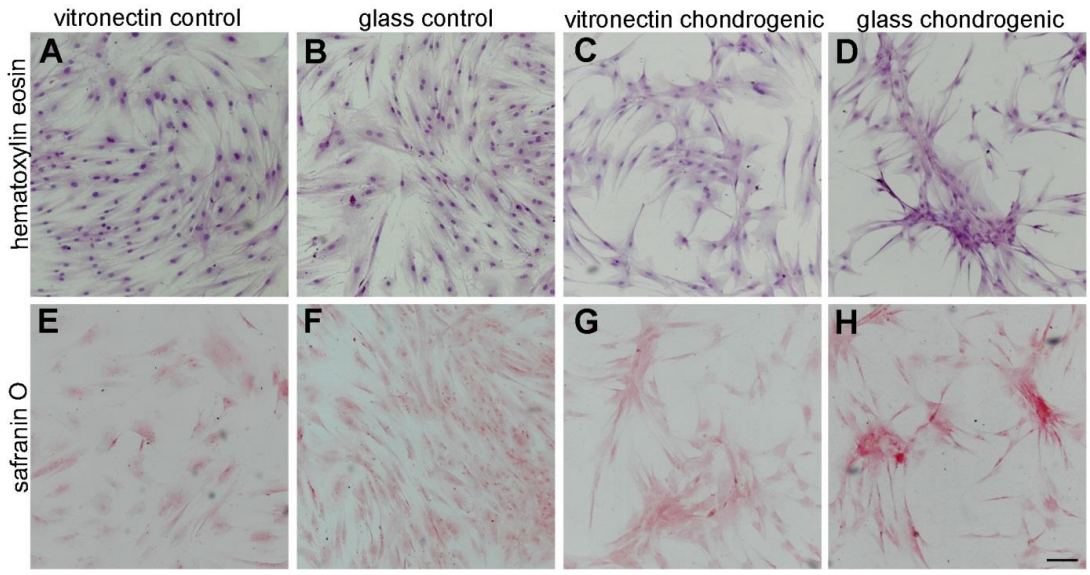


**Fig. 4. bMSCs in control and on day 7 of chondrogenic commitment plated on glass and vitronectin substrates**

*A-D – Hematoxylin-eosin staining, E-H – Staining with safranin O, bar 50 μm. Chondrogenic differentiation is more rapid for glass –plated cells*

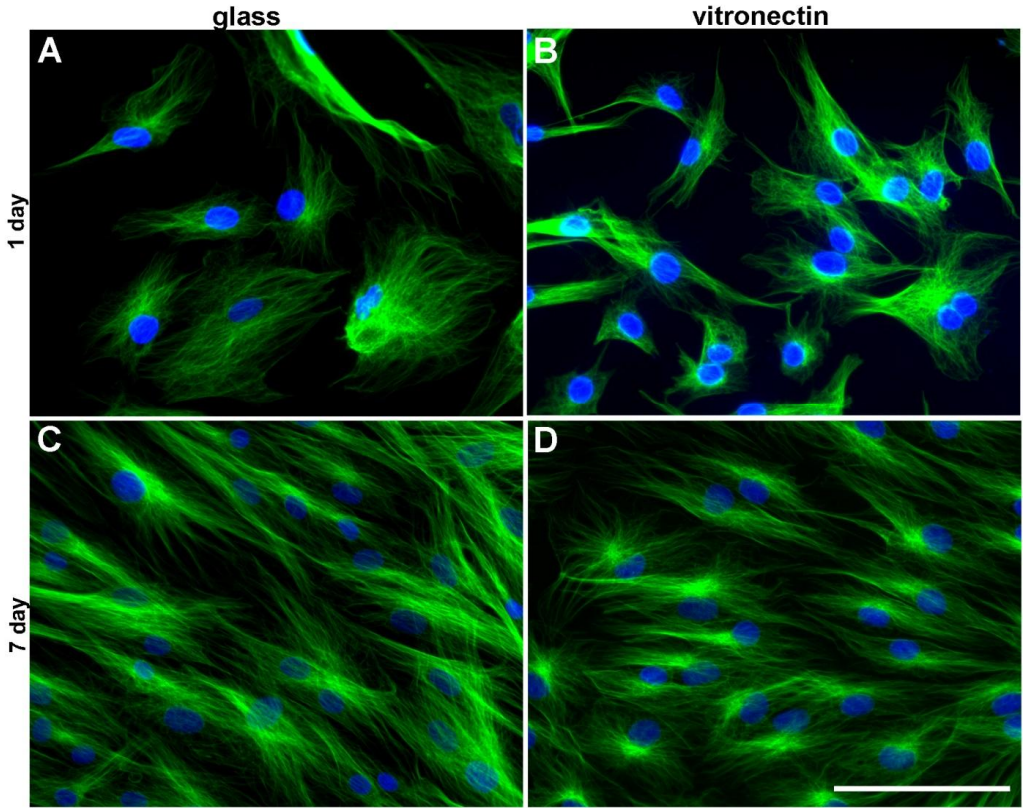


**Fig. 5. Visualization of MT array for control cells and on day 7 of chondrogenic differentiation**

*Microtubules are presented in green pseudocolor, nuclei are counterstained with DAPI (blue), bar 50 μm. A-B – first day, C-D day 7 of the chondrogenic commitment*

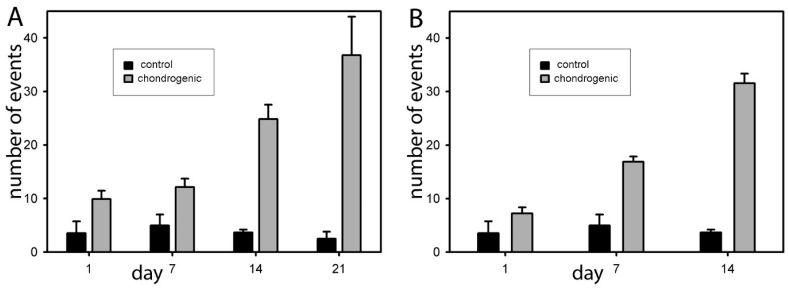


**Fig. 6. Increase of cells with the non-radial MT array during chondrogenic differentiation, data are presented as mean±SD**

*A – Cells plated on vitronectin, B – Cells plated on glass*

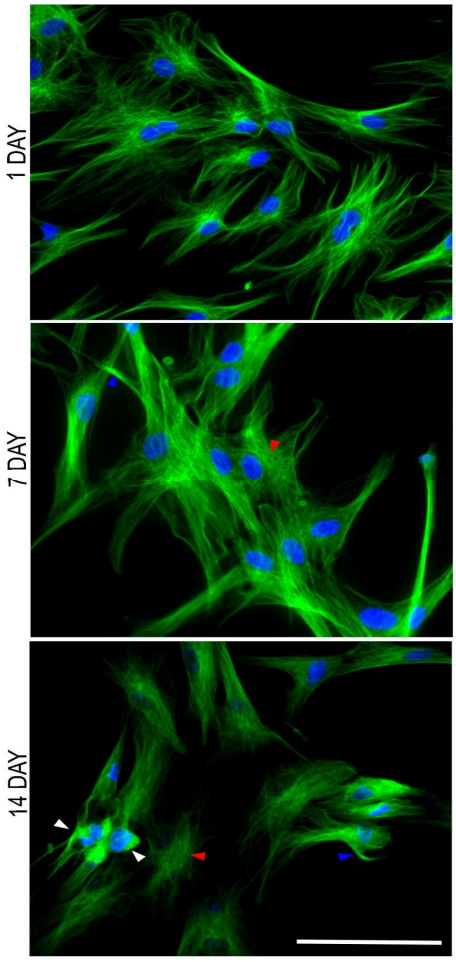


**Fig. 7. Changes of MT array from day 1 to day 14 of chondrogenic differentiation for cells plated on glass**

*Microtubules are presented in green pseudocolor, nuclei are counterstained with DAPI (blue), bar 50 μm. Red triangles point on chaotic network of non-centrosomal MTs, blue triangles point on the thick bundles of MTs near the cell edge, white triangles point on basket-like MT structures around the nucleus*

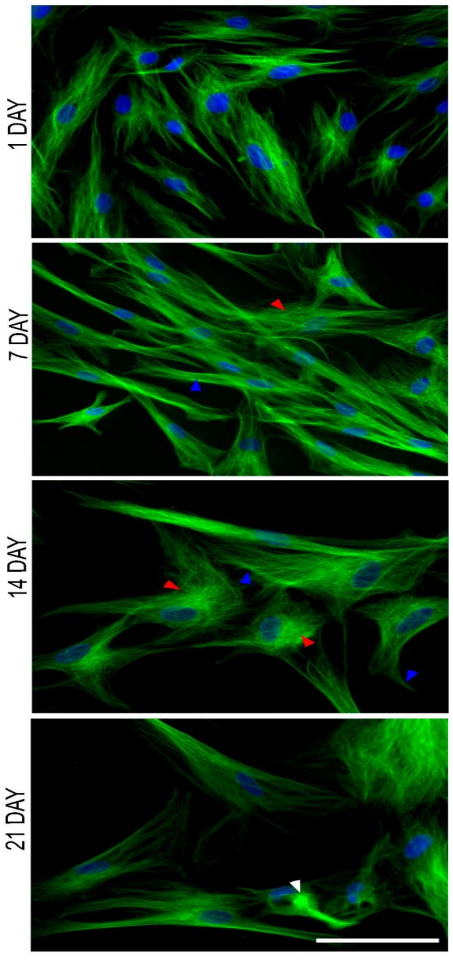


**Fig. 8. Changes of MT array from day 1 to day 21 of chondrogenic differentiation for cells plated on vitronectin**

*Microtubules are presented in green pseudocolor, nuclei are counterstained with DAPI (blue), bar 50 μm. Red triangles point on chaotic network of non-centrosomal MTs, blue triangles point on the thick bundles of MTs near the cell edge, white triangles point on basket-like MT structures around the nucleus*

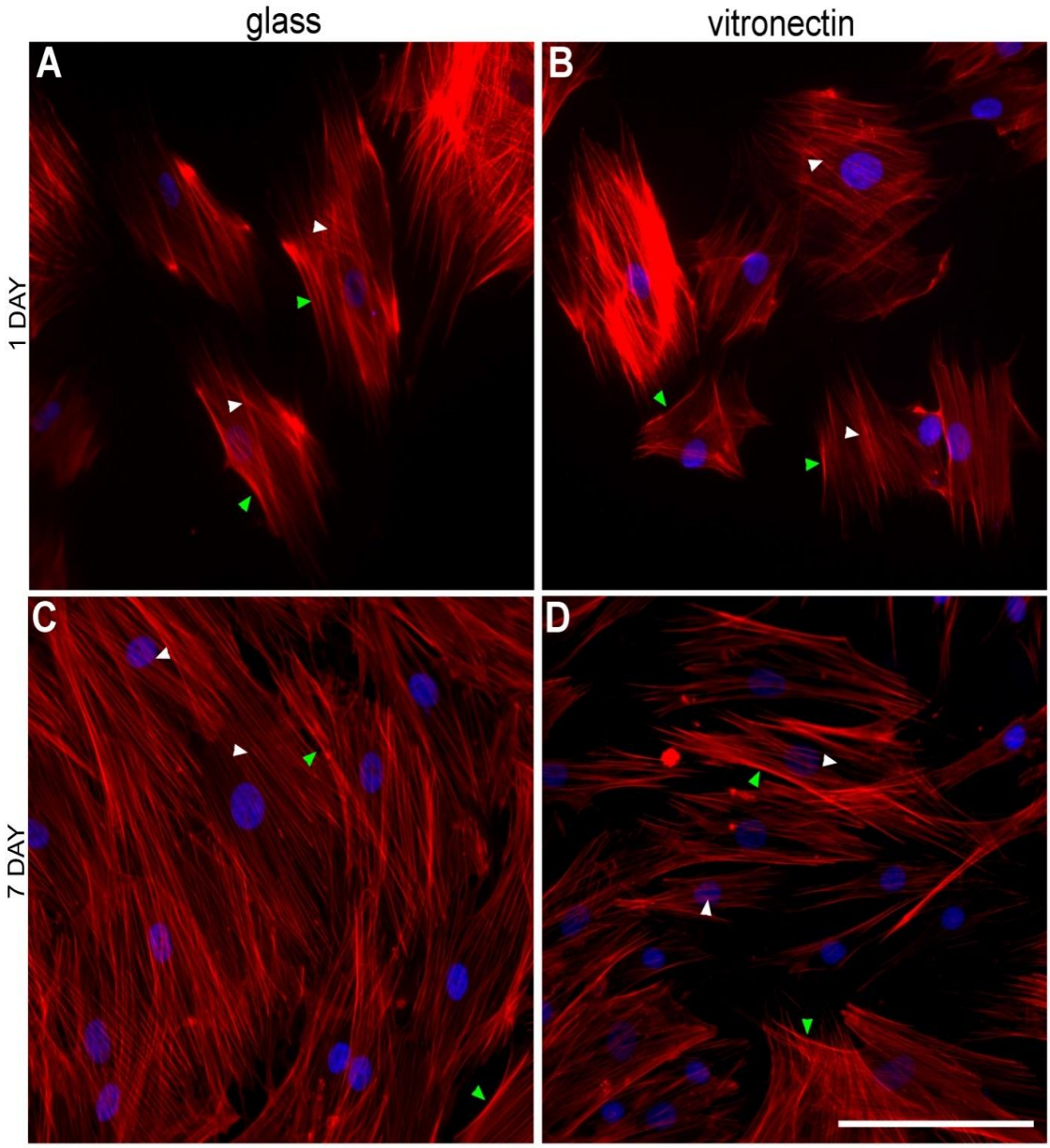


**Fig. 9. Visualization of actin structures for control cells and on day 7 of chondrogenic differentiation**

*Actin filaments are presented in red pseudocolor, nuclei are counterstained with DAPI (blue), bar 50 μm. A-B – first day, C-D - day 7 of the chondrogenic commitment. Green triangles point on the actin arches, white triangles point on the stress fibers*

The direct evidence on the role of actin components in chondrogenic differentiation was provided by Lim et al. [32] on chick wing-bud MCS. They showed that disruption of the actin cytoskeleton with cytochalasin D encouraged chondrogenesis by activating PKCalpha downregulation of ERK signaling. Actin cytoskeleton network can also be disrupted indirectly by the inhibition of RhoA pathway with Y27632. Murine limb-bud MSC after the incubation with Y27632 expressed high levels of glycosaminoglycans, became rounded and form a thin network of cortical actin [33]. There is no direct evidence for the role of microtubule network in response to mechanistic stimuli during chondrogenesis. However, MTs might play a role

in MCSs during the osteogenic differentiation [12]. MCSs treated with high concentrations of nocodazole in osteogenic conditions rapidly changed their shape from an elongated spindle-like to the characteristic shape of differentiated osteoblasts with long protrusions, that implied the additive effect of microtubule disruption during this process.

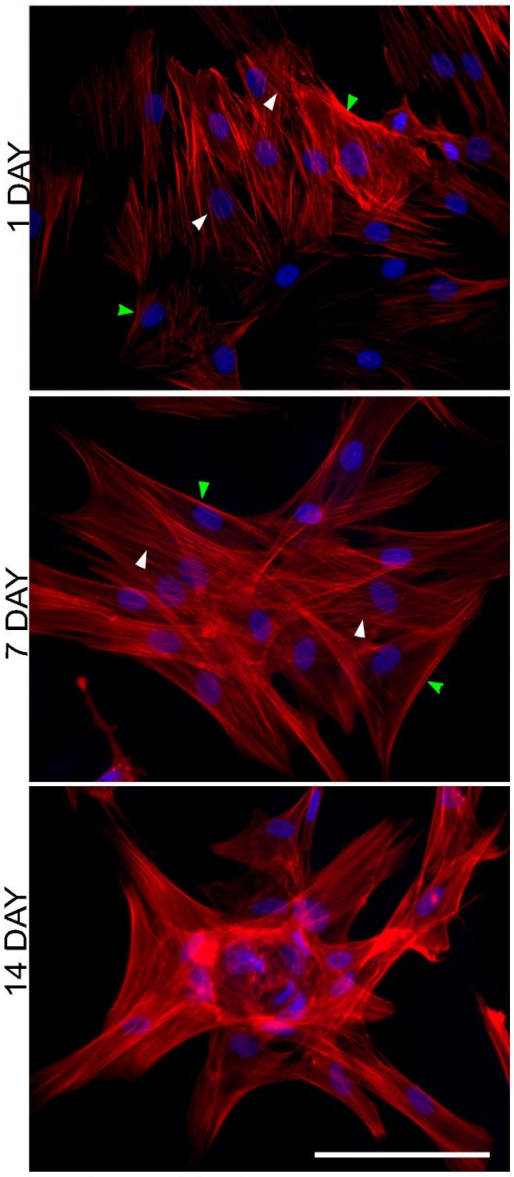


**Fig. 10. Changes of actin structures from day 1 to day 14 of chondrogenic differentiation for cells plated on glass**

*Actin filaments are presented in red pseudocolor, nuclei are counterstained with DAPI (blue), bar 50 μm. Green triangles point on the actin arches, white triangles point on the stress fibers*

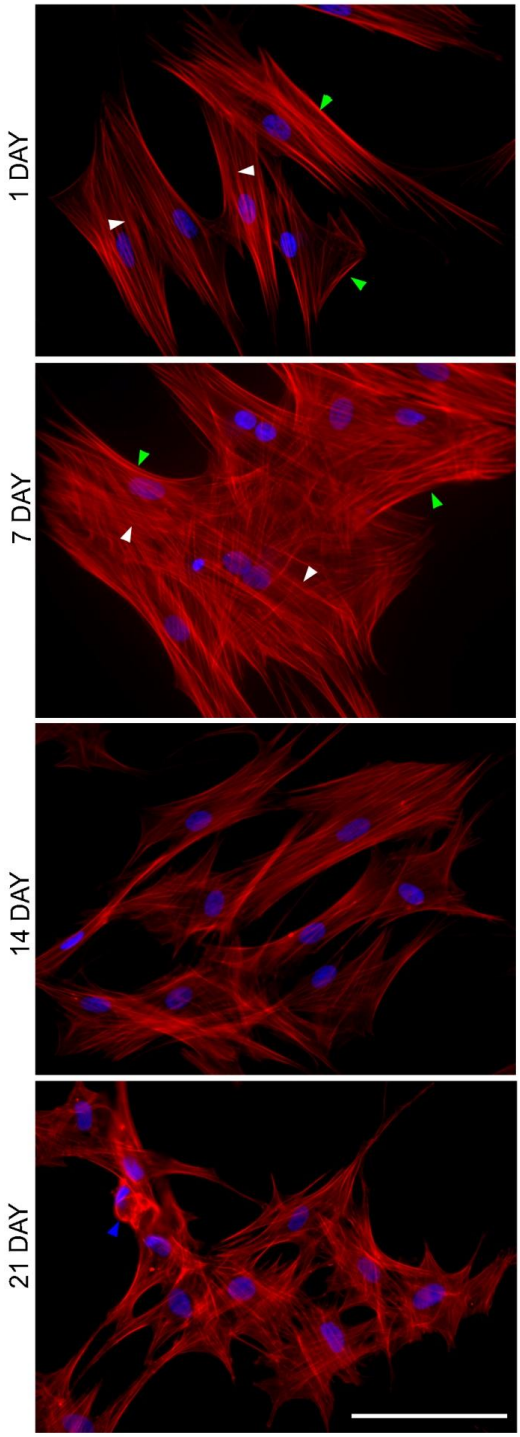


**Fig. 11. Changes of actin structures from day 1 to day 21 of chondrogenic differentiation for cells plated on vitronectin**

*Actin filaments are presented in red pseudocolor, nuclei are counterstained with DAPI (blue), bar 50 μm. Green triangles point on the actin arches, white triangles point on the stress fibers*

In our study, we described the morphological changes of MT and actin network during the chondrogenic differentiation of bovine MSCs. Firstly, the chondrogenic differentiation of MSCs depended on the substrate type and occurred more rapidly on the non-specific glass substrate than in the presence of integrin-specific ligands on vitronectin. These data are consistent with the studies that report the disruption of actin network in chondrogenesis since in the presence of integrin ligands MCSs might form the focal adhesions, which in turn promote the formation of stress fibers and thus decreasing the rate of chondrogenesis. Secondly, we have shown that the cell area decreases during the chondrogenesis process and cells become more elongated. The main changes of actin structures in differentiating chondrocytes include the disappearance of stress fibers and thick actin arches, so actin network in differentiated chondrocytes can be described as a thin network of the cortical actin that was also confirmed by other groups (18-21). Thirdly, we have shown for the first time that organization of MT network is also disrupted during chondrogenesis process. The main changes of MT network during chondrogenesis of MSC are the disruption of the radial pattern that is characteristic for all fibroblast-like cells and the presence of numerous non-centrosomal microtubules that grow transversely to the cell radius. The gradual increase of non-radial MTs leads to the formation of basket-like MT structures that were previously described for differentiated chondrocytes [34, 35]. The dynamic parameters of the MT network during the chondrogenic differentiation are still a subject for further investigation. Our data show the important role of two cytoskeleton systems for the differentiation of MCS on a bovine model.

## 5. CONCLUSION

Our results suggest that redistribution of cytoskeletal components during chondrogenic differentiation of bovine MSCs plays a major mechanistic role in this process. These findings are important for the field of stem cell biology in general and cartilage regeneration assays in particular, as much is known about the biochemical and molecular events during stem cell differentiation, and very little is known about the direct physical processes. Our data will have wide implications in the field of tissue engineering and development of new bio-materials that potentiate the desired changes of cytoskeleton to enhance the differentiation capacities of the target cells.

## COMPETING INTERESTS

Authors have declared that no competing interests exist.

## REFERENCES

1. Friedenstein AJ, Chailakhjan RK, Lalykina KS. The development of fibroblast colonies in monolayer cultures of guinea-pig bone marrow and spleen cells. Cell Tissue Kinet. 1970;3:393-403.
2. Lara E, Rivera N, Rojas D, Rodriguez-Alvarez LL, Castro FO. Characterization of mesenchymal stem cells in bovine endometrium during follicular phase of oestrous cycle. Reprod Domest Anim. 2017;52:707-14.
DOI: 10.1111/rda.12969
3. Sampaio RV, Chiaratti MR, Santos DC, Bressan FF, Sangalli JR, Sa AL, Silva TV, Costa NN, Cordeiro MS, Santos SS, Ambrosio CE, Adona PR, Meirelles FV, et al. Generation of bovine (*Bos indicus*) and buffalo (*Bubalus bubalis*) adipose tissue derived stem cells: Isolation, characterization, and multipotentiality. Genet Mol Res. 2015;14:53-62.
DOI: 10.4238/2015.January.15.7
4. Chang LB, Peng SY, Chou CJ, Chen YJ, Shiu JS, Tu PA, Gao SX, Chen YC, Lin TK, Wu SC. Therapeutic potential of amniotic fluid stem cells to treat bilateral ovarian dystrophy in dairy cows in a subtropical region. Reprod Domest Anim. 2018;53:433-41.
DOI: 10.1111/rda.13123
5. Cardoso TC, Okamura LH, Baptistella JC, Gameiro R, Ferreira HL, Marinho M, Flores EF. Isolation, characterization and immunomodulatory associated gene transcription of Wharton's jelly-derived multipotent mesenchymal stromal cells at different trimesters of cow pregnancy. Cell Tissue Res. 2017;367:243-56.
DOI: 10.1007/s00441-016-2504-9
6. Rossi B, Merlo B, Colleoni S, Iacono E, Tazzari PL, Ricci F, Lazzari G, Galli C. Isolation and *in vitro* characterization of bovine amniotic fluid derived stem cells at different trimesters of pregnancy. Stem Cell Rev. 2014;10:712-24.
DOI: 10.1007/s12015-014-9525-0
7. Corradetti B, Meucci A, Bizzaro D, Cremonesi F, Lange Consiglio A. Mesenchymal stem cells from amnion and amniotic fluid in the bovine. Reproduction. 2013;145:391-400.

DOI: 10.1530/rep-12-0437
8. Pittenger MF, Mackay AM, Beck SC, Jaiswal RK, Douglas R, Mosca JD, Moorman MA, Simonetti DW, Craig S, Marshak DR. Multilineage potential of adult human mesenchymal stem cells. Science. 1999;284:143-7.
9. Duenas F, Becerra V, Cortes Y, Vidal S, Saenz L, Palomino J, De Los Reyes M, Peralta OA. Hepatogenic and neurogenic differentiation of bone marrow mesenchymal stem cells from abattoir-derived bovine fetuses. BMC Vet Res. 2014;10:154.
DOI: 10.1186/1746-6148-10-154
10. Marletta G, Ciapetti G, Satriano C, Perut F, Salerno M, Baldini N. Improved osteogenic differentiation of human marrow stromal cells cultured on ion-induced chemically structured poly-epsilon-caprolactone. Biomaterials. 2007;28:1132-40.
DOI: 10.1016/j.biomaterials.2006.10.027
11. Munoz-Pinto DJ, Jimenez-Vergara AC, Hou Y, Hayenga HN, Rivas A, Grunlan M, Hahn MS. Osteogenic potential of poly(ethylene glycol)-poly(dimethylsil-oxane) hybrid hydrogels. Tissue Eng Part A. 2012;18:1710-9.
DOI: 10.1089/ten.TEA.2011.0348
12. Rodriguez JP, Gonzalez M, Rios S, Cambiazo V. Cytoskeletal organization of human mesenchymal stem cells (MSC) changes during their osteogenic differentiation. J Cell Biochem. 2004;93: 721-31.
DOI: 10.1002/jcb.20234
13. Sen B, Uzer G, Samsonraj RM, Xie Z, McGrath C, Styner M, Dudakovic A, van Wijnen AJ, Rubin J. Intranuclear actin structure modulates mesenchymal stem cell differentiation. Stem Cells. 2017;35:1624-35.
DOI: 10.1002/stem.2617
14. Yourek G, Hussain MA, Mao JJ. Cytoskeletal changes of mesenchymal stem cells during differentiation. Asaio J. 2007;53:219-28.
DOI: 10.1097/MAT.0b013e31802deb2d
15. Meka SRK, Chacko LA, Ravi A, Chatterjee K, Ananthanarayanan V. Role of microtubules in osteogenic differentiation of mesenchymal stem cells on 3D nanofibrous scaffolds. ACS Biomaterials Science & Engineering. 2017;3:551-9.
DOI: 10.1021/acsbiomaterials.6b00725
16. Hayakawa K, Sato N, Obinata T. Dynamic reorientation of cultured cells and stress fibers under mechanical stress from periodic stretching. Exp Cell Res. 2001; 268:104-14.
DOI: 10.1006/excr.2001.5270
17. De R, Zemel A, Safran SA. Theoretical concepts and models of cellular mechanosensing. Methods Cell Biol. 2010;98:143-75.
DOI: 10.1016/s0091-679x(10)98007-2
18. Mathieu PS, Loboa EG. Cytoskeletal and focal adhesion influences on mesenchymal stem cell shape, mechanical properties, and differentiation down osteogenic, adipogenic, and chondrogenic pathways. Tissue Eng Part B Rev. 2012;18:436-44.
DOI: 10.1089/ten.TEB.2012.0014
19. Borjesson DL, Peroni JF. The regenerative medicine laboratory: Facilitating stem cell therapy for equine disease. Clin Lab Med. 2011;31:109-23.
DOI: 10.1016/j.cll.2010.12.001
20. Meirelles Lda S, Fontes AM, Covas DT, Caplan AI. Mechanisms involved in the therapeutic properties of mesenchymal stem cells. Cytokine Growth Factor Rev. 2009;20:419-27.
DOI: 10.1016/j.cytogfr.2009.10.002
21. Peroni JF, Borjesson DL. Anti-inflammatory and immunomodulatory activities of stem cells. Vet Clin North Am Equine Pract. 2011;27:351-62.
DOI: 10.1016/j.cveq.2011.06.003
22. Lee KB, Hui JH, Song IC, Ardany L, Lee EH. Injectable mesenchymal stem cell therapy for large cartilage defects--a porcine model. Stem Cells. 2007;25:2964-71.
DOI: 10.1634/stemcells.2006-0311
23. Mauck RL, Yuan X, Tuan RS. Chondrogenic differentiation and functional maturation of bovine mesenchymal stem cells in long-term agarose culture. Osteoarthritis Cartilage. 2006;14:179-89.
DOI: 10.1016/j.joca.2005.09.002
24. Cortes Y, Ojeda M, Araya D, Duenas F, Fernandez MS, Peralta OA. Isolation and multilineage differentiation of bone marrow mesenchymal stem cells from abattoir-derived bovine fetuses. BMC Vet Res. 2013;9:133.
DOI: 10.1186/1746-6148-9-133
25. Vandesompele J, De Preter K, Pattyn F, Poppe B, Van Roy N, De Paepe A, Speleman F. Accurate normalization of real-time quantitative RT-PCR data by geometric averaging of multiple internal control genes. Genome Biol. 2002;3.

26. Erickson IE, van Veen SC, Sengupta S, Kestle SR, Mauck RL. Cartilage matrix formation by bovine mesenchymal stem cells in three-dimensional culture is age-dependent. Clin Orthop Relat Res. 2011; 469:2744-53.
DOI: 10.1007/s11999-011-1869-z
27. Bosnakovski D, Mizuno M, Kim G, Ishiguro T, Okumura M, Iwanaga T, Kadosawa T, Fujinaga T. Chondrogenic differentiation of bovine bone marrow mesenchymal stem cells in pellet cultural system. Exp Hematol. 2004;32:502-9.
DOI: 10.1016/j.exphem.2004.02.009
28. Bosnakovski D, Mizuno M, Kim G, Takagi S, Okumura M, Fujinaga T. Chondrogenic differentiation of bovine bone marrow mesenchymal stem cells (MSCs) in different hydrogels: Influence of collagen type II extracellular matrix on MSC chondrogenesis. Biotechnol Bioeng. 2006; 93:1152-63.
DOI: 10.1002/bit.20828
29. Huang CY, Hagar KL, Frost LE, Sun Y, Cheung HS. Effects of cyclic compressive loading on chondrogenesis of rabbit bone-marrow derived mesenchymal stem cells. Stem Cells. 2004;22:313-23.
DOI: 10.1634/stemcells.22-3-313
30. Kupcsik L, Stoddart MJ, Li Z, Benneker LM, Alini M. Improving chondrogenesis: Potential and limitations of SOX9 gene transfer and mechanical stimulation for cartilage tissue engineering. Tissue Eng Part A. 2010;16:1845-55.
DOI: 10.1089/ten.TEA.2009.0531
31. Park JS, Chu JS, Tsou AD, Diop R, Tang Z, Wang A, Li S. The effect of matrix stiffness on the differentiation of mesenchymal stem cells in response to TGF-beta. Biomaterials. 2011;32: 3921-30.
DOI: 10.1016/j.biomaterials.2011.02.019
32. Lim YB, Kang SS, Park TK, Lee YS, Chun JS, Sonn JK. Disruption of actin cytoskeleton induces chondrogenesis of mesenchymal cells by activating protein kinase C-alpha signaling. Biochem Biophys Res Commun. 2000;273:609-13.
DOI: 10.1006/bbrc.2000.2987
33. Woods A, Beier F. RhoA/ROCK signaling regulates chondrogenesis in a context-dependent manner. J Biol Chem. 2006;281:13134-40.
DOI: 10.1074/jbc.M509433200
34. Idowu BD, Knight MM, Bader DL, Lee DA. Confocal analysis of cytoskeletal organisation within isolated chondrocyte sub-populations cultured in agarose. Histochem J. 2000;32:165-74.
35. Langelier E, Suetterlin R, Hoemann CD, Aebi U, Buschmann MD. The chondrocyte cytoskeleton in mature articular cartilage: Structure and distribution of actin, tubulin, and vimentin filaments. J Histochem Cytochem. 2000;48:1307-20.
DOI: 10.1177/002215540004801002




*Peer-review history:*
*The peer review history for this paper can be accessed here:*
*http://www.sciencedomain.org/review-history/27925*